Third Cycle in Astronomy : THE SOLAR WIND (16 December 1975) - M. ROTH

9.- Interaction of the solar wind with the earth's magnetic field

1. Introduction

It is well established now that a continual radial outflow of plasma from the sun, reaches the neighbourhood of the Earth with a supersonic speed of about 400 km/sec. This solar wind plasma will obviously interact with the terrestrial magnetic field of dipolar origin.

A schematic illustration of this interaction is shown in Figure 1, which represents the noon-midnight magnetic meridian plane. As a result the magnetic field is confined within an elongated cavity which deflects the solar wind around it. Usually the point of closest approach of the solar wind is at a geocentric radial distance of about 10 R_E in the upstream direction. At this stagnation point, the flow speed vanishes. On the other hand, as the velocity of the solar wind near the Earth is greater than the propagation speed of any hydromagnetic wave in the medium, a bow shock wave develops upstream. It is similar in many ways to the bow shock wave ahead of a round-nosed projectile or vehicle in supersonic flight. In the dayside, the geocentric distance to the subsolar point of the shock is about 14 to 15 earth radii during quiet conditions.

Satellites and space probes have identified a transition region of compressed subsonic plasma flow, immediately behind the shock ahead of the Earth. In this region the plasma density and temperatures are increased. The energy of the solar wind particles is almost entirely in the form of random thermal motions, and the bulk velocity is very low. However, as the plasma flows away from the stagnation point, it accelerates and energy is transferred from thermal to directed motion. A sonic surface is reached, in the position indicated by the dashed line, and thereafter

the flow is further accelerated, eventually becoming highly supersonic more. At great distances from the Sun-Earth axis the shock wave is attenuated and slightly deflects the solar wind. The transition region between the bow shock and the terrestrial magnetic field is called the magnetosheath. This region acts like an elastic medium transmitting the kinetic pressure of the solar wind onto the earth's magnetic field. The field confines this field to a well defined cavity called the magnetosphere. Downstream from the Earth, the magnetosphere stretches out to form an extended tail within which the magnetic field is directed away from the Earth in the southern hemisphere and toward the Earth in the northern hemisphere. Within the tail and separating the regions of opposite field polarity, we find the magnetic equatorial neutral sheet (not shown in the figure), and a substantially thicker region which contains drifting particles. A thin boundary layer, the magnetopause separates the magnetosheath from the magnetosphere.

In the early theories of the magnetosphere by Chapman and Ferraro (1), the interplanetary magnetic field was ignored, and the magnetopause was consequently the outermost surface of closed field lines, in effect by definition. All the magnetic field lines on this surface radiated from a region about N_s in the southern high latitude dayside region, and reentered back into the magnetosphere through a similar point N_n in the north.

However, the addition of the interplanetary magnetic field means that the field strength at the high latitude regions never vanishes, and the word neutral is strictly speaking not appropriate. With the observations by Frank (2), that magnetosheath plasma does indeed penetrate down to low altitudes, through these regions, the so-called dayside polar cusps. Further observations showed that the cross-sectional area of the penetrating plasma column is large, being some 1° to 4° in north-south extent. Accordingly, a term such as magnetic cleft

proposed by Heikkila (3), seems more appropriate. These clefts are located at geomagnetic latitudes of about 70-75° and at geocentric radial distances of approximately 10 R_E, in the dayside region.

Recently, plasma measurements in the distant polar magnetosphere, tailward of the cusps by Paschmann et al.(4) and later Rosenbauer et al.(5) have revealed the presence of a persistent layer of plasma, adjacent to the magnetopause, and enveloping, tailward of the cusps, the entire magnetosphere. For this reason, this layer has been called, by Rosenbauer et al.(5), the plasma mantle. Its thickness varies between about 0.5 R_E and 4.0 R_E and the layer comprises magnetosheath plasma, flowing away from the cusps into the magnetotail, along magnetic lines of force adjacent to the magnetopause, but inside the magnetosphere. The fact that the plasma mantle is not observed on the dayside of the magnetosphere, equatorward of the polar cusps, leads to the conclusion, that this portion of the dayside magnetopause acts as an effective barrier, against the direct entry of magnetosheath plasma.

2. The structure of the Ferraro magnetopause

Most early studies of the interaction between the solar wind and the geomagnetic field treated the magnetosphere as a vacuum and ignored the weak interplanetary magnetic field embedded in the solar plasma. The first paper on the small-scale, internal structure of the magnetopause was written in 1952 by Ferraro (6). Long before this however, from 1931 till 1941, he collaborated with Chapman in a famous series of papers (1 - 7 - 8 - 9 - 10) on the origin of geomagnetic storms. They introduced, amongst many new ideas, the basic concept of a sharp boundary layer, the magnetopause in modern terminology, between the compressed geomagnetic field and discrete plasma streams flowing almost radially outwards from the Sun. Today, these pioneering investigations remain fundamental to all theoretical studies of the magnetopause.

As the thickness of the magnetopause is presumably negligible compared with its radius of curvature, Ferraro made the assumption that each element of this boundary could be treated as a plane for a first approximation.

With this assumption, Ferraro, and later Rosenbluth (11) considered the steady-state situation (figure 2) in which a stream of ions and electrons with equal concentrations and bulk velocities, is incident normally on a unidirectional magnetic field. The ions and electrons are assumed to be devoid of thermal motions, and thus all particles of the same type have the same orbit, which is essentially rectilinear in the main body of the stream where the magnetic field is assumed vanishing. As the ions and electrons enter the increasing magnetic field in the boundary layer, they are deflected transversely in opposite senses. This transverse motion of the particles generates an electric current parallel to the boundary layer. The particles are bent around in the boundary layer until they re-enter the main body of the stream with a reflected velocity equal and opposite to their incident velocity. Because of their greater mass-to-charge ratio, the positive ions tend to penetrate more deeply into the magnetic field than the electrons.

The tendency for the ions and electrons to separate produces a polarization electric field perpendicular to the boundary layer. This electric field opposes the charge separation so that the ions and electrons move approximately together perpendicularly to the boundary layer. Therefore, the charge separation remains small. The ions are reflected in the boundary layer primarly by the polarization electric field rather than by the magnetic deflecting force, and thus their trajectories bend around sharply. The incident electrons, however, are accelerated by the electric field and deflected by the magnetic field until they attain a maximum kinetic energy nearly equal to the original kinetic energy of the ions. Thus the electric field transfers energy from the ions to the electrons. In this way the electrons acquire a large transverse velocity parallel to the boundary layer

that greatly exceeds that of the ions. Therefore, the current is carried predominantly by the electrons. The reflected electrons are decelerated by the electric field, and their energy is transferred back to the reflected ions.

In the fluid, or macroscopic steady state description of the boundary layer, the electromagnetic body force, acting on the current is balanced by the pressure gradient force of the plasma :

$$\frac{dp}{dx} = jB \qquad (1)$$

where p is the pressure of the plasma force, j is the current density, B the magnetic field, and x denotes a distance measured normally to the boundary layer (see figure 2) and directed into the stream.

The Maxwell equation, $\text{rot } \vec{B} = \mu_o \vec{j}$ (MKSA units), becomes an one dimensional equation (due to the assumption of a plane boundary layer) :

$$\frac{dB}{dx} = - \mu_o j \qquad (2)$$

Eliminating j between equation (1) and (2), the result can be integrated directly to give

$$p + \frac{B^2}{2 \mu_o} = \text{constant} \qquad (3)$$

This important equation (3) expresses the constancy of total pressure, kinetic + magnetic, throughout the plane boundary layer.

By the assumption that the interplanetary magnetic field is negligible on the solar side of the boundary layer, and that the magnetospheric plasma pressure is negligible on the terrestrial side, the equilibrium occurs when the plasma pressure on the solar side, $p^{s.s}$, balances the magnetic

pressure on the magnetospheric side : $(B^2/2\ \mu_o)^{m.s}$, so that at the magnetopause :

$$p^{s.s} = (B^2/2\ \mu_o)^{m.s} \qquad (4)$$

The surface current, flowing in the boundary layer, has the right sens, to shield the interior of the plasma, from the vacuum magnetic field, so that in the Ferraro model, the magnetic field reduces well to zero on the plasma side of the plane surface current, and is exactly twice the unperturbed field on the other. However, if the geomagnetic field is represented by a magnetic dipole, the magnetic field is only exactly twice the unperturbed field, on the line joining the dipole and its image in the plane interface (12).

The solution obtained by Ferraro and Rosenbluth, using the charge neutral approximation in the plasma- and fields equations, show that the magnetic field, the electric current and the polarization electric field, all decrease exponentially within the stream, with a well-defined characteristic distance.

This characteristic scale distance may however be deduced by simple physical considerations if we try to obtain an indication of the current sheath thickness (Phelps : 13).

If d is this current sheath thickness (see figure 2), the Maxwell equation (2) can be written on the form :

$$\frac{\overline{B}}{d} = -\mu_o\ j \qquad (5)$$

The bar on physical quantities denotes an average over the thickness of the layer. If we neglect the ion current, the current j contains only the electronic component :

$$j = - n_e \, e \, \overline{v}_y \qquad (6)$$

n_e is the number density of the incident particles, e is the proton charge, and $\overline{v}_y$ is the mean velocity of the electrons transversely to the layer (figure 2), y being a distance measured in the direction of the current.

This velocity can be estimated by the following physical considerations. To a first approximation, neglecting the electric field in the x-direction, the electrons experience a mean y - component of force which is essentially the Lorentz force :

$$\overline{F} = e \, \overline{U} \, \overline{B} \qquad (7)$$

where U is the normal component of velocity of the incident electrons.

By Newton's law, this force is also the change of momentum by unit time :

$$\overline{F} = m_e \, \overline{v}_y / \tau \qquad (8)$$

where τ is the time the electron has passed in the boundary and m_e is the electron's mass. This time is :

$$\tau = \frac{2 \, d}{\overline{U}} \qquad (9)$$

The factor 2 comes from the fact that the particles are reflected in the layer. Eliminating τ between equations (8) and (9) and equaling the result with equation (7), one deduces an estimation for $\overline{v}_y$:

$$\overline{v}_y = 2 \, d. \frac{e \, \overline{B}}{m_e} \qquad (10)$$

Combining equations ( ), (6) and (10), the characteristic length d writes down immediately

$$d = \left(\frac{m_e}{2 \mu_o n_e e^2} \right)^{1/2} \qquad (11)$$

Equation (11) takes also the form

$$d = \frac{c}{\omega_p} \qquad (12)$$

where ω_p is the electron plasma frequency.

$$\omega_p = \left(\frac{N_e e^2}{m_e \varepsilon_o} \right)^{1/2} \qquad (13)$$

N_e is the total number density of electrons comprising both incident and reflected particles ($N_e = 2 n_e$). d is called the electron skin depth (e.s.d). It is thus a natural unit of length in the study of boundary layers between plasmas and magnetic fields, or between different kinds of plasma, immersed in a magnetic field.

Furthermore, as it is assumed that all the solar particles incident on the boundary layer have zero temperature, the total pressure on the geomagnetic field is the product of the change of momentum by the flux of plasma :

$$p = 2 n (m_i + m_e) U^2 \qquad (14)$$

n is the density of the incident particles of either sign, (since the solar

wind plasma is macroscopicly neutral : $n = n_e = n_i$), m_e and m_i being the electrons and ions masses.

Neglecting the momentum of the electrons and eliminating the density between the equilibrium relation (4) and the equation (11) defining d, we obtain :

$$d = \sqrt{2}\left(\frac{m_e U}{eB}\right)^{1/2} \cdot \left(\frac{m_i U}{eB}\right)^{1/2} = \sqrt{2}\, R_e\, R_i \qquad (15)$$

This equation shows that, for the case of a cold plasma incident on a initially constant magnetic field, the electron skin depth is just the geometric mean of the cyclotron radii of the electrons (R_e) and ions (R_i), having energies equal to their incident kinetic energies in the (maximum) magnetic field just outside the boundary, on the vacuum side.

The e.s.d. can also be expressed in a suitable form for numerical calculations by the relation :

$$d = 5.3 / \sqrt{N_e} \qquad (16)$$

where the total electron number density, N_e, is expressed in cm^{-3} and d in km.

As the number electron density in the magnetosheath, at the nose of the magnetopause, has a typical value of 30 particles per cm^{-3}, the e.s.d is of the order of 1 km. The Ferraro magnetopause is then defined as the thin boundary layer in which the bulk of the shielding current flows. Its thickness is at most a few multiples of the e.s.d.

In the approach of Ferraro (6), analytical solutions were obtained using the charge neutral approximation. In this approximate treatment, because of their electrostatic attraction, the ions and electrons moved strictly together and were turned back simultaneously at the same point in

space. But in an exact treatment, Sestero (14) and, later, Davies (15) found that the separation distance δ (figure 2) between the position of deepest penetration of the ions and electrons is of the order of the Debye length :

$$\delta \sim \left(\frac{\varepsilon_o m_e U^2}{N_e e^2} \right)^{1/2} \qquad (17)$$

For U = 300 km/s and N_e = 30 cm^{-3}, we find δ = 1 m. Thus δ is much smaller than d.

The more deeply penetrating protons produce a surface layer of positive charges whose thickness is only of the Debye length. The repartition of the charges is shown schematically at right of the figure 2. The negative charge has its maximum value at the electron turning point and decreases rapidly exponentially within the stream, with a characteristic scale distance of the order of the electron skin depth.

3. The shape of the magnetopause

The results for the idealized plane boundary layer are unaltered if the magnetosheath particles, have an initial component of velocity that is parallel to the plane boundary layer, but is still perpendicular to the magnetic field, because this transverse component of velocity is unchanged by the reflection process. Therefore, the particle pressure arising from specular reflection is given by

$$p = 2\, n(m_i + m_E)\, U^2 \cos^2 \phi \qquad (18)$$

where ϕ is the angle between the inward normal to the magnetopause ($\vec{n}$) and the incident velocity.

It follows that the three-dimensional pressure-balance condition :

$$2\ n\ (m_i + m_e)\ U^2\ \cos^2\ \psi = B^2/2\ \mu_o \qquad (19)$$

generalizes the equation (4).

This equation remains valid when the magnetopause is in motion if the components of velocity are now referred to a local frame of reference in which the magnetopause is instantaneously at rest. This equation shows that B, the magnetospheric magnetic field adjacent to the magnetopause varies with position if ψ varies with position on the magnetopause.

Using this pressure balance condition, several iterative methods have been developed for finding the shape of the magnetopause. The method introduced by Mead and Beard (16) is particularly simple and convenient to use.

In a first approximation, the magnetic field due to the currents flowing at the magnetopause surface is neglected and the magnetic field at the boundary is twice that of the geomagnetic dipole field. Then, a first surface is calculated. From this approximate surface, the electrical currents everywhere on the surface are deduced (from the (modified) Maxwell equation : $\mu_o\ \vec{j} = \vec{n}\ \Lambda\ \vec{B}$) The field correction due to the departure of the surface from a local plane is calculated by integrating the Biot-Savart integral of these currents over this first approximate surface. This correction is added to the initial field and the corrected field is reintroduced into the pressure balance condition. The cycle is repeated until no change in the surface is obtained on successive iterations. The figure 3 is a pictorial view of the magnetopause computed by this method by Midgley and Davis (17). As the magnetic field is found very sensitive to small differences of boundary shape, particularly at the neutral points, the entire surface, at each cycle, must be computed at about 1600 points (the

density of points being the largest at the neutral points). The fourth iteration is usually adequate.

4. Departures from the simple model

The idealized model of Ferraro for the magnetopause boundary involves some drastic assumptions and simplifications.

For example, the thermal motions of the incident ions and electrons are ignored and it is usually assumed that no particles are trapped in the magnetopause. Furthermore the plasma is heated on passing through the bow shock wave and may be turbulent in the magnetosheath. Neglecting the thermal motions of the incident particles is certainly invalid near the stagnation point, at the nose of the magnetopause, where the flow of the plasma is subsonic and the thermalization the greatest. In addition, small dynamic perturbations of the magnetopause may cause some particles, particularly electrons, to become trapped within the boundary layer. As Grad (18) has pointed out, the absence of trapped particles corresponds to the thinnest possible sheath. If trapped particles are allowed then, there is no unique solution. In the macroscopic description, any pressure and magnetic field profiles satisfying the equilibrium equation define an allowable equilibrium solution. Some related problems have been discussed by Longmire (19) who shows that in some cases, for example if the velocity distribution deep inside the plasma is Maxwellian, there is no solution without trapped particles.

A further complication is that the magnetosphere is not a vacuum but is populated by thermal and energetic charged particles.

5. The Parker's magnetopause

As suggested by Parker (20-21-22), ambient thermal electrons and ions are available at the magnetopause to neutralize the polarization electric field, because the magnetic lines of force linking the magnetopause pass through the polar cusps, or magnetospheric clefts down to the ionosphere. The ionosphere acts then as an essentially unlimited reservoir of thermal particles having relatively high mobility across the lines of force. The modifications in the structure of the boundary layer are shown in figure 4.

If the electrostatic field at the magnetopause is completely neutralized, the impinging magnetosheath ion and electron streams move independently of each other, and every particle penetrates into the geomagnetic field a distance approximately equal to its cyclotron radius. In the steady state, there is no transfer of energy from the ions to the electrons and the bulk of the electric current is carried by the ions as a result of their much larger cyclotron radius. Figure 4 shows also the distribution of excess solar charges, resulting from the deeper penetration of the magnetosheath ions, and the neutralizing distribution of ambient magnetospheric charges.

The magnetic field decreases almost exponentially within the ion layer with a characteristic scale distance D which is just the average cyclotron radius of an ion in the magnetopause until the electron turning point is reached (23-24). For representative magnetosheath parameters D is of the order of 100 km. Thereafter the magnetic field decreases almost exponentially with a characteristic scale distance, the e.s.d.(d) of the order of 1 km.

However, complete neutralization of the polarization electric field is unlikely not obtained because the solar wind pressure fluctuates continually. Under time-varying conditions, it is necessary to compare the

time constant for variations of the charge density, arising from a change in the solar wind pressure, with the time constant for the neutralization of the electrostatic field. An estimation of this latter time constant has been obtained by Willis (25), using an idealized magnetosphere-ionosphere circuit analogue (figure 5). In this approach the two geomagnetic flux tubes linking the magnetopause to the ionosphere are treated as lossless, coaxial transmission lines. The ionospheric terminations are represented by resistive annular disks, ant the magnetopause by a simple capacitor. After an abrupt increase in the pressure of the solar wind, the classical boundary layer of Ferraro is formed very rapidly, and polarization charges are induced at the magnetopause (fig. 5). Willis (25) has calculated that the relaxation of this system takes a few hours to discharge by current flow through the ionosphere. This relatively long time constant suggests that the electrostatic field may not be completely neutralized, since the solar wind pressure does not usually remain constant for as long as an hour.

6. The geomagnetic tail

Figure 6 represents an artist's conception, due to Heikkila (26), of the magnetosphere, its plasma populations and associated boundaries.

An important property of the nightside current system, flowing around the flanks of the magnetosphere, in the magnetopause,and closing itself through the neutral sheet, is that it produces a perturbation magnetic field directed toward the sun above the earth's equatorial plane, and away from the sun below this plane. Thus the perturbation field increases the magnetic flux on the nightside, confining the tail to its cylindrical shape.

7. The role of the interplanetary magnetic field

Some of the most pressing questions regarding the general configuration of the magnetosphere are concerned with the interplanetary magnetic field line connection across the magnetopause, and the mechanism of transfer of particles, energy, and momentum from the solar wind to the magnetosphere. All these problems are, of course, intimately linked with the analysis of the detailed structure and dynamics of the magnetopause. There is mounting evidence from studies of the rapid access of solar flare protons into the magnetosphere (27) that the open field lines emerging from the polar cusps must somewhere cross the magnetopause and link up with the interplanetary magnetic field that flows past the boundary, embedded in the solar wind (figure 6).

Figure 7 from Dessler (28) shows the model of reconnection or merging, first suggested by Dungey (29) in 1961.

When the interplanetary magnetic field (IMF) turns southwards (as field line 1" in fig. 7) the opposite magnetospheric and solar wind fields merge or reconnect at a neutral point at the nose of the magnetosphere (fig. 7 : 2"-2'). In this theory, the magnetic energy lost by annihilation of opposite magnetic fields at the neutral point is converted into kinetic energy of motion to the solar wind, which is then deflected around the nose of the magnetosphere. In the frozen field convection concept, the motion of the solar wind carries the plasma on the reconnected interplanetary field line, and hence the field line itself, tailward. As the two halves of the field line move tailward in the interplanetary medium (sequence of field lines 2" to 6" in fig. 7), the magnetospheric part of the lines, each of which has a foot in one polar cap, also moves tailward (sequence of field lines 2' to 6' in fig. 7). Eventually, the two halves of the line merge or reconnect in the tail at a neutral point (fig. 7 : 7"-7'), again forming a magnetospheric field line with two feet on the ground (8') and an interplanetary field line (8") not connected with the Earth. The newly connected field line (8'), then

moves earthward to return to the dayside merging region to repeat this process all over again.

Moving field lines, while a useful concept for some, are totally irrelevant to others, and hence the above model is viewed with some suspicion. However, there is really no basic difficulty, since the field lines have no identity in the sense of string or spaghetti and it is entirely equivalent to view the field lines in this model as stationary and talk entirely in terms of plasma motions (blank arrows in fig. 7). The solar wind plasma flows across the interplanetary field lines. When it encounters the magnetosphere, it mixes with an outward flow from the magnetosphere. The magnetopause is not a perfect conductor in this model, and part of the interplanetary electric field induced by the motion of solar plasma across the interplanetary magnetic field, penetrates into the polar field lines and causes a tailward flow in this region (see for example Vasyliunas (30) for a review of the merging theory). Flows over the north and south polar caps eventually meet in the tail. Then some of the plasma flows earthward and some tailward. It must also be said (30) that the process of merging or reconnection of magnetic field lines may take place, only when there is an electric field component along the X-line. (A characteristic of the interconnected magnetic fields (30-31) is that there is a singular line or separatrix, not a field line, which defines the boundary of closed field lines. For the special case of a strictly southward IMF (Fig. 7), the separatrix is an X-type neutral line, or more accurately an X-ring, completely around the magnetosphere. The magnetic field strength at the line vanishes, and the field lines in the plane normal to this neutral line form an X geometry (see the neutral points in fig. 7). In the more general case, where the IMF has an arbitrary orientation there are two neutral points, more or less on opposite sides of the magnetosphere ; these are joined by two separatrices, which are now X-lines with a tangential component of magnetic field along them. The projection of the field lines on a plane normal to the X-line still shows an X-type geometry. The essential feature of an X-line, is that there is no component of magnetic field perpendicular to it,

and therefore no Lorentz force acts on a charged particle moving along it.

For some, the interplanetary magnetic field represents the external driving mechanism of the magnetospheric electric field. If the magnetic field lines are electric potentials everywhere, it is possible to map this external electric field into the magnetosphere down to the polar ionosphere (32), if one knows exactly the manner in which the magnetic field lines are connected through the magnetopause and this leads to the well-known magnetospheric dawn-dusk electric field in the equatorial plane outside the plasmasphere.

8. Other mechanisms for transfering energy from the solar wind to the magnetosphere

At the present time, it is not at all clear, whether the IMF is the sole external cause of the magnetospheric electric field. The existence of a dawn-dusk electric field and associated convection pattern, at all times in the magnetosphere, as introduced by Axford and Hines (33), regardless of the characteristics of the interplanetary magnetic field, suggests the coexistence of another (or even several) steady-state, external driving mechanism, which in the theory of Axford (34) would be caused by a viscous interaction or "tangential drag" of the solar wind magnetosheath plasma with the magnetospheric plasma. This interaction, taking place at the magnetopause, would be sufficient to drive the convection magnetospheric plasma deep within the magnetosphere.

The existence of some mechanism for the transfer of energy from the solar wind to the upper atmosphere has been established from studies of the effects of atmospheric drag on the orbits of Earth satellites at relatively low altitudes (35-36-37). This transfer of energy is explained in terms of a solar wind-magnetosphere interaction (38). Indeed, the steady-state heating produced by the currents in the polar ionosphere, as

described for example in Willis theory (25), is directly proportional to the velocity of the solar wind. Thus, to the extend that the geomagnetic activity is related to this velocity, the corpuscular heating of the upper atmosphere is also. And, consequently, there is always some atmospheric heating by the solar wind, because there is always some drag, or dissipative effect, on the geomagnetic cavity.

Recently (1974), a new approach to the study of the magnetopause has been introduced by Cole (39). This author has used the adiabatic theory of charged particles motion (40) to examine the reflection of magnetosheath particles (figure 8) at a plane magnetopause for the case in which the surfaces of constant magnetic intensity are inclined at a large angle to this magnetopause. In figure 8, corresponding to the equatorial dawn side, a proton enters the magnetosphere at O with guiding centre at C_o and exists the magnetosphere at D with guiding centre at C_D. It can be seen that the reflection is no more specular and that the transverse component of particle momentum parallel to the magnetopause is changed during the reflection process. Furthermore, Cole has demonstrated that incident magnetosheath particles making an angle with the magnetopause which is less than a critical value can penetrate into the geomagnetic field quite freely. By this process, protons are captured on the dawn side and electrons on the dusk side, leading again to the well known dawn-dusk electric field. The capture of these magnetosheath particles causes also a "tangential drag" on the geomagnetic field. Adiabatic theory (40) is questionable to discuss the motion of charged particles across the magnetopause since the magnetic field changes appreciably over distances comparable with the ion cyclotron radius. Nevertheless, the imaginative ideas outlined by Cole warrant further research and it would be interesting to consider these new concepts within the framework of the self consistent plasma-fields equation of a kinetic theory, without resorting to the guiding centre approximation.

9. Experimental observations

Theoretical predictions of the location and shape of the magnetopause based on an analogy with continuum gas dynamics are in reasonably good agreement with the observations : the average geocentric distance of the magnetopause near the noon-magnetic meridian is about 10 R_E and this distance increases to about 12-14 R_E near the dawn and dusk meridians.

In general, however, it is found that the measurements are not yet sufficiently detailed to distinguish reliably between the competing theoretical models for the magnetopause structure. This is due to the fact that the magnetopause is a very thin layer that is usually in motion and it is considerably more difficult to deduce the small-scale, internal structure, from traversals by a single satellite, than to determine merely the location of the magnetopause. Figure 9 is a magnetometer record of the geomagnetic field obtained near the noon meridian by Explorer 12 on September 13, 1961 (41). The magnitude of the total magnetic intensity is plotted against geocentric distance from the Earth. The smooth curve shows the variation of the intensity with distance for the Finch and Leaton (42) geomagnetic reference field. Also plotted are the angles α and ψ, defining the orientation of the field relatively to the spin axis of the satellite and to the Sun. It can be seen that the magnetopause is characterized by a sudden, large change in field direction. It is accompanied by a reduction in field magnitude and increased fluctuations in the direction and magnitude of the field in the magnetosheath. In can also be seen, that the field strength just inside the magnetosphere is about twice the strength of the dipole field in agreement with the theory.

A salient feature of many satellite traversals is that the magnetopause appears to be crossed repeatedly in a single pass (multiple crossings) which suggests that this boundary is frequently in motion (43-44-45-46). The spatial amplitudes of the motion vary from about 0.2 to 2.2 R_E and the motion is sometimes periodic. The characteristic times

of the motion usually vary from 2 to 15 minutes (47-48), but both longer periods (49-50) and shorter periods (46) are sometimes observed.

The precise thickness of the magnetopause is difficult to determine experimentally because of the motion of this boundary. Cahill and Patel (44) have found that the thickness on the dayside is usually in the range 20 to 300 km, while Heppner et al. (45) have estimated experimentallythat the thickness of the dayside magnetopause is about 100 km, 200 km being a likely upper limit. Other measurements (43-46) have confirmed that the thickness of the dayside part of the magnetopause is generally of the order of 100 km, which is comparable to the proton cyclotron radius in the boundary layer. The magnetopause is still a well-defined boundary at the orbit of the Moon (51) and beyond (52). At the lunar distance, the thickness of the magnetopause is usually about 1000 km, but sometimes only 30 km (51). These estimates for the thickness of the magnetopause are all comparable to, or greater than, the proton cyclotron radius ; they imply that the electrostatic field at the magnetopause is usually negligible, for otherwise the thickness of the magnetopause would be only of the order of 1 km, as in the Ferraro model (6).

The magnetometer data have also been analyzed in an attempt to determine the vector normal to the magnetopause and the component of magnetic field in this direction (53-54). The observations suggest that two distinct types of boundary structure exist : a tangential discontinuity, in which the field magnitude sometimes has a minimum value within the current layer and is usually different on either side of the layer ; and a rotational discontinuity, in which the magnitude of the magnetic field remains constant but the direction changes on crossing from the magnetosphere into the magnetosheath. A tangential discontinuity corresponds to the boundary layer discussed by Ferraro (6) and Parker (20-21-22). A rotational discontinuity however has a component of magnetic field normal to the boundary, and the magnitude of this component provides some indication of the amount of field-

line interconnection at the magnetopause (the interconnection implies that there is a normal component of magnetic field at the magnetopause that permits the interpenetration of magnetosheath and magnetosphere plasmas by the process of field-aligned diffusion).

Although the shape and location of the magnetopause are now fairly well understood in terms of analogies with continuum gas dynamics, the detailed, internal structure of the magnetopause remains uncertain. Most of the measurements are able to determine the location of the magnetopause because the physical characteristics on either side of the magnetopause are usually quite distinct. The time resolution of the measurements, however, is inadequate to provide a detailed survey in the interior of such a thin (about 100 km) boundary layer. For this reason, theoretical studies of the magnetopause structure have often proceeded without strict reference to experimental observations.

The early studies were based on an investigation of individual particle orbits and neglected, among other factors, the thermal motions of the incident particles, the possible existence of trapped particles in the boundary layer, turbulence in the magnetosheath, the interplanetary magnetic field, and the presence of ambient magnetospheric and ionospheric plasma. More recent studies have attempted to take account of some of these factors, but, the simultaneous inclusion of all these complicating factors presents a formidable problem that has not yet been studied.

10. The geomagnetic activity

At the present time, our knowledge of the interaction of the solar wind with the magnetosphere can provide us plausible mechanisms to explain certain aspects of the geomagnetic activity.

For example, it is possible to predict geomagnetic activity up to two hours in advance by using in situ interplanetary measurements.

Burton et al. (55) have predicted the Dst index using in situ measurements of the solar wind velocity, number density and interplanetary field strength. Figure 10 shows the result of this prediction for a moderately disturbed period (March 3, 4 and 5, 1968). The top panel is the square root of the dynamic pressure, the middle panel, the square of the westward solar magnetospheric component of the interplanetary electric field times its sign. The solid line at the bottom panel is the measured Dst index during this period. The dashed line is the predicted Dst. It can be seen that there is a good agreement between calculated and observed Dst.

The philosophy of this calculation is the following : Burton et al. (55-see also : Russell, 56) have used interplanetary observations during ten magnetic storms to derive an empirical expression for the rate of change of Dst. The calculation proceeds as follows :

$$Dst'(t) = Dst(t) - a\sqrt{mn(t)\ V^2(t)} + b \qquad (20)$$

$$\frac{\partial}{\partial t}\,(Dst'(t)) = -\,c\,E_W^2\,(t-\tau) - d\,Dst'(t) \qquad (21)$$

$$Dst\ (t+\Delta) = Dst(t) + \Delta\,\frac{\partial}{\partial t}\,(Dst'(t)) \qquad (22)$$

Where m is the proton mass, n the number density and V the velocity of the solar wind. E_W is the east-west component of the interplanetary $(\vec{V} \wedge \vec{B})$ electric field, set equal to zero if E_W is negative or eastwards (or when the IMF is northwards), and τ is a time lag for magnetospheric response. In these expression, Dst is in γ ($1\ \gamma = 10^{-5}$ G $= 10^{-9}$ Wb/m^2), P $= mnV^2$ in eV m^{-1}. The constants used in constructing figure 10 from equations (20) to (22) are : a equals 0.18 γ (eV.cm^{-3})$^{-1/2}$; b equals 16 γ ; d equals 3.5×10^{-5} s^{-1} ; and c equals 4.4×10^{-4} γ (mV.m^{-1})$^{-2}$ s^{-1}. The response time τ, of the

magnetosphere to the interplanetary electric field has been held constant at 30 min in this study and it is shown that these constants work equally well on quiet days as well as disturbed.

The first equation (20) corresponds to the initial phase of magnetic storms during which the excess of the solar wind pressure exerted on the magnetosphere, leads to a sudden increase of the magnetic field. Dst' is then a new Dst index from which the contribution of the solar wind dynamic pressure has been removed. The second equation (21) corresponds to the main phase of the magnetic storm during which the magnetic field intensity is decreased due to the increase of the ring current intensity. It is assumed that the main phase development rate is proportional to the square of the dawn-dusk or east-west component of the interplanetary electric field E_W. The change in Dst is added to the initial Dst value in the third equation (22).

At the present time, there is some evidence that the southward component of the interplanetary magnetic field is the causative agent of the geomagnetic activity and it appears that the previously found relations between geomagnetic activity and solar wind velocity although real do not necessarily result from a causative effect of the solar wind velocity on geomagnetic activity but are probably due to correlations between the various solar wind parameters (57). Figure 11 from Russell et al. (58) shows the solar wind number density and velocity, the interplanetary magnetic field strength and solar magnetospheric north-south component, measured on Explorer 33, in the solar wind, on March 3, 1968. In the bottom two panels are the Dst and AE indices for the same time period. The apparent cause of the strengthening of the ring current, measured by a decrease of about 30 γ in Dst, after 1600 UT, was the strong southward component of the interplanetary magnetic field at 1500 UT. No change is seen in the solar wind number density, velocity or magnetic field strength. On the other hand, the magnetic field is predominantly southward on this day.

Another manifestation of the control of magnetospheric dynamics by the southward component of the interplanetary magnetic field is the semiannual variation of geomagnetic activity (57). This semiannual variation can be seen in all indices of geomagnetic activity. Figure 12 from Russell and McPherron (57) shows the semiannual variation as determined from storm counts data of Chapman and Bartels (59) and by using the Dst index (57). The left panel is the occurence of great storms and smaller storms from 1875 to 1927. The right panel is the occurence of storms with Dst less than -40, -80, and -160 γ during the years 1958 and 1961 through 1969. The semiannual variation has maximums at spring and fall, and a 2 to 1 enhancement of equinoctial to solstitial storm occurence. The explanation has been given by Russell and McPherron (57) : The interplanetary magnetic field is ordered in the solar equatorial (GSEQ) coordinates system rather than solar ecliptic (GSE) coordinates (see the appendix for a description of coordinates systems). The interaction of the southward component of the interplanetary field with the magnetosphere is ordered in the solar magnetospheric (GSM) coordinates system. These coordinates systems all have a common X-axis which points at the sun, but the Y-and Z-axes differ by a rotation about the X-axis. The angles between the GSEQ and GSM axes are a function of both time of day and day of year, while the angles between the GSEQ and GSE axes are a function of day of year only. A possible relative orientation of these three systems is shown in figure 13.

A field along the idealized spiral would have an X- and Y-components in the GSEQ system, but no Z- component. Since the coordinates systems all have a common X-axis, the X-component is the same in each system. However, as is illustrated in figure 13, even an idealized spiral field can have a southward component in the other coordinate systems. Since, the magnetosphere interacts more strongly with southward fields than with northward fields, because the merging rate is greater, the varying relative orientation of the GSEQ and GSM coordinates systems, during the rotation of the Earth around the Sun, gives a semiannual variation of the probability of a southward

component in solar magnetospheric coordinates. The interaction is proportional to the strength of the southward component and there is no interaction for northward fields. Finally, it can be shown that the model of Russell and McPherron (57) explains also the annual variation, the 11- and 22- Yr cycles in geomagnetic activity but does not furnish an explanation for the diurnal variation (60-61).

Many authors have found diurnal variations of geomagnetic activity. The question is whether these variations are due to ionospheric effects or whether they are controlled by the solar-wind magnetosphere interaction. Vercheval (62) has found that the existence of a daily density variation in the mean thermosphere could be associated with a lack of symmetry in the configuration of the geomagnetic field. Because of the rotation of the dipole around the axis of rotation of the Earth, a component of the daily variation of the geomagnetic activity is generated. This component of the geomagnetic activity is known as the McIntosh (63) component. The variation is a time universal effect, thus presenting a planetary character. This daily variation would be due to a preferential orientation of the dipole axis for the energy storage responsible of the geomagnetic effect.

Appendix : Geophysical coordinates systems (from Russell - 64)

1. Geocentric solar magnetospheric system (GSM)

The GSM system has its X-axis from the Earth to the Sun. Tye Y-axis is defined to be perpendicular to the Earth's magnetic dipole so that the X-Z plane contains the dipole axis. The positive Z-axis is chosen to be in the same sens as the nothern magnetic pole.

2. Geocentric solar equatorial system (GSEQ)

The GSEQ system has its X-axis pointing towards the Sun from the Earth. However, instead of having its Y-axis in the ecliptic plane, the GSEQ Y-axis is parallel to the Sun's equatorial plane which is inclined to the ecliptic. We note that since the X-axis is in the ecliptic plane and therefore is not necessarily in the Sun's equatorial plane, the Z-axis of this system will not necessarily be parallel to the Sun's axis of rotation. However, the Sun's axis of rotation must lie in the X-Z plane. The Z-axis is chosen to be in the same sense as the ecliptic pole, i.e. northwards.

3. Geocentric solar ecliptic system (GSE)

The GSE system has its X-axis pointing from the Earth towards the Sun and its Y-axis is chosen to be in the ecliptic plane pointing towards dusk (thus opposing planetary motion). Its Z-axis is parallel to the ecliptic pole. Relatively to an inertial system, this system has a yearly rotation.

REFERENCES

Most part of this notes has been inspired from reviews of :

- ROEDERER, J.G., 1974. The Earth's Magnetosphere, Science, 183 (4120), 37-46.
- RUSSELL, T.R., 1974. The solar wind and magnetospheric dynamics, in "Correlated Interplanetary and Magnetospheric Observations", 3-47, Ed. D.E. Page, D. Reidel, Dordrecht, Netherlands.
- WILLIS, D.M., 1971. Structure of the Magnetopause, Rev. Geophys. Space Phys., 9, 953-985.
- WILLIS, D.M., 1975. The Microstructure of the Magnetopause, Geophys. J. R. Astr. Soc., 41, 355-389.

Specific references are listed below :

1. CHAPMAN, S. and FERRARO, V.C.A., 1931. A new theory of magnetic storms : Part I - The initial phase, Terr. Magn. atmos. Elect., 36, 77-97, 171-186.
2. FRANK, L.A., 1971. Plasma in the earth's polar magnetosphere, J. Geophys. Res., 76, 5202-5219.
3. HEIKKILA, W.J., 1972. The morphology of auroral particle precipitation, Space Research, 12, 1343-1355, eds. S.A. Bowhill, L.D. Jaffe and M.J. Rycroft, Akademic-Verlag, Berlin.
4. PASCHMANN, G., GRUNWALDT, H., MONTGOMERY, M.D., ROSENBAUER, H. and SCKOPKE, N., 1974. Plasma observations in the high-latitude magnetosphere, in "Correlated Interplanetary and Magnetospheric Observations", 249-253, ed. D.E. Page, D. Reidel, Dordrecht, Netherlands.
5. ROSENBAUER, H., GRUNWALDT, H., MONTGOMERY, M.D., PASCHMANN, G. and SCKOPKE, N., 1975. Heos 2 plasma observations in the distant polar magnetosphere - the plasma mantle, J. Geophys. Res., 80, 2723-2737.

6. FERRARO, V.C.A., 1952. On the theory of the first phase of a geomagnetic storm : a new illustrative calculation based on an idealized (plane not cylindrical) model field distribution, J. Geophys. Res., 57, 15-49.

7. CHAPMAN, S. and FERRARO, V.C.A., 1932. A new theory of magnetic storms. Part I - The initial phase, Terr. Magn. atmos. Elect., 37, 147-156, 421-429.

8. CHAPMAN, S. and FERRARO, V.C.A., 1933. A new theory of magnetic storms : Part II - The main phase, Terr. Magn. atmos. Elect., 38, 79-96.

9. CHAPMAN, S. and FERRARO, V.C.A., 1940. The theory of the first phase of a geomagnetic storm, Terr. Magn. atmos. Elect., 45, 245-268.

10. CHAPMAN, S. and FERRARO, V.C.A., 1941. The geomagnetic ring current : I - Its radial stability, Terr. Magn. atmos. Elect., 46, 1-6.

11. ROSENBLUTH, M.N., 1954. Los Alamos Laboratory Report LA-1850. Later reprinted in "Magnetohydrodynamics", 57-66, ed. R. Landshoff, Stanford University Press.

12. DUNGEY, J.W., 1958. In "Cosmic Electrodynamics", 137-146, Cambridge University Press, London.

13. PHELPS, A.D.R., 1973. Interactions of plasmas with magnetic field boundaries, Planet. Space Sci., 21, 1497-1509.

14. SESTERO, A., 1965. Charge separation effects in the Ferraro-Rosenbluth cold plasma sheath model, Phys. Fluids, 8, 739-744.

15. DAVIES, C.M., 1967. Charge separation effects in the Ferraro-Rosenbluth cold plasma sheath model, Phys. Fluids, 10, 391-395.

16. MEAD, G.D. and BEARD, D.B., 1964. Shape of the geomagnetic field solar wind boundary, J. Geophys. Res., 69, 1169-1179.

17. MIDGLEY, J.E. and DAVIS, L., Jr., 1963. Calculation by a moment technique of the perturbation of the geomagnetic field by the solar wind, J. Geophys. Res., 68, 5111-5123.

18. GRAD, H., 1961. Boundary layer between a plasma and a magnetic field, Phys. Fluids, 4, 1366-1375.

19. LONGMIRE, C.L., 1963. In "Elementary Plasma Physics", Chapt. V, 90-107, Interscience, New York.

20. PARKER, E.N., 1967. Confinement of a magnetic field by a beam of ions, J. Geophys. Res., 72, 2315-2322.

21. PARKER, E.N., 1967. Small-scale non equilibrium of the magnetopause and its consequences, J. Geophys. Res., 72, 4365-4374.

22. PARKER, E.N., 1968. Dynamical properties of the magnetosphere, in "Physics of the Magnetosphere", ed. R.L. Carovillano, J.F. McClay and H.F. Radoski, 3-64, D. Reidel, Dordrecht, Netherlands.

23. BEARD, D.B., 1967. The solar wind, Rep. progr. Phys., 30, part 2, 409-444.

24. BEARD, D.B. and CHOE, J.Y., 1974. The magnetospheric boundary, in "Correlated Interplanetary and Magnetospheric Observations", 97-114, ed. D.E. Page, D. Reidel, Dordrecht, Netherlands.

25. WILLIS, D.M., 1970. The electrostatic field at the magnetopause, Planet. Space Sci., 18, 749-769.

26. HEIKKILA, W.J., 1972. Penetration of particles into the polar cap regions of the magnetosphere. In "Critical Problems of Magnetospheric Research", ed. E.R. Dyer, 67-82 (IUCSTP, Secretariat National Academy of Sciences, Washington).

27. MORFILL, G. and SCHOLER, M., 1973. Study of the Magnetosphere Using Energetic Solar Particles, Space Sci. Rev. 15, 267-349.

28. DESSLER, A.J., 1968. Solar wind interactions and the magnetosphere, in "Physics of the Magnetosphere", 65-105, ed. R.L. Carovillano, J.F. McClay and H.R. Radoski, D. Reidel, Dordrecht, Netherlands.

29. DUNGEY, J.W., 1961. Interplanetary magnetic field and the auroral zones, Phys. Rev. Lett., 6, 47-48.

30. VASYLIUNAS, V.M., 1975. Theoretical Models of Magnetic Field Line Merging, 1, Rev. Geophys. Space Phys., 13, 303-336.

31. HEIKKILA, W.J., 1975. Magnetospheric Plasma Regions and Boundaries, paper (reprint) presented at Nobelsymposium on the Physics of the Hot Plasma in the Magnetosphere, April 2-4, Kiruna, Sweden.

32. STERN, D.P., 1973. A study of the electric field in an open magnetospheric model, J. Geophys. Res., 78, 7292-7305.

33. AXFORD, W.I. and HINES, C.O., 1961. A Unifying theory of high-latitude geophysical phenomena and geomagnetic storms, Can. J. Phys., 39, 1433-1464.

34. AXFORD, W.I., 1964. Viscous interaction between the solar wind and the earth's magnetosphere, J. Geophys. Res., 67, 3791-3796.

35. MacDONALD, G.J.F., 1963. The Escape of Helium from the Earth's Atmosphere, Rev. Geophys., 1, 305-349.

36. JACCHIA, L.G., SLOWEY, J. and VERNIANI, F., 1966. Geomagnetic Perturbations and Upper Atmosphere Heating, Smithsonian Astrophys. Obs. Spec. Rep. n° 218.

37. MOE, K., 1967. The Corpuscular Heating Effect Observed by Explorer 6 near Sunspot Minimum, Planetary Space Sci., 15, 1821-1827.

38. COLEMAN, P.J., Jr., 1970. Tangential drag on the geomagnetic cavity, Cosmic Electrodynamics, 1, 145-159.

39. COLE, K.D., 1974. Outline of a theory of solar wind interaction with the magnetosphere, Planet. Space Sci., 22, 1075-1088.

40. NORTHROP, T.G., 1963. The Adiabatic Motion of Charged Particles, Interscience Publishers, New York.

41. CAHILL, L.J. and AMAZEEN, P.J., 1963. The boundary of the geomagnetic field, J. Geophys. Res., 68, 1835-1843.

42. FINCH, H.F. and LEATON, B.R., 1957. The Earth's main magnetic field-epoch 1955.0, Mon. Notic. Roy. Astron. Soc., Geophys. Suppl., 7, 314-317.

43. HOLZER, R.E., McLEOD, M.G. and SMITH, E.J., 1966. Preliminary Results from the Ogo 1 search coil magnetometer : Boundary positions and magnetic noise spectra, J. Geophys. Res., 71, 1481-1486.

44. CAHILL, L.J., Jr. and PATEL, V.L., 1967. The boundary of the geomagnetic field, August to November 1961, Planet. Space Sci., 15, 997-1033.

45. HEPPNER, J.P., SUGIURA, M., SKILLMAN, T.L., LEDLEY, B.G. and CAMPBELL, M., 1967. Ogo 1 magnetic field observations, J. Geophys. Res., 72, 5417-5471.

46. AUBRY, M.P., KIVELSON, M.G. and RUSSELL, C.T., 1971. Motion and structure of the magnetopause, J. Geophys. Res., 76, 1673-1696.

47. ANDERSON, K.A., BINSACK, J.H. and FAIRFIELD, D.H., 1968. Hydromagnetic disturbances of 3 to 15 minutes period on the magnetopause and their relation to bow shock spikes, J. Geophys. Res., 73, 2371-2386.

48. SMITH, E.J. and DAVIS, M., Jr., 1970. Magnetic measurements in the earth's magnetosphere and magnetosheath : Mariner 5, J. Geophys. Res., 75, 1233-1245.

49. FREEMAN, J.W., Jr., KAVANAGH, L.D., Jr. and CAHILL, L.J., Jr., 1967. An observation of transient variations in the magnetospheric boundary position, J. Geophys. Res., 72, 2040-2044.

50. KAUFMANN, R.L. and KONRADI, A., 1969. Explorer 12 magnetopause observations : Large-scale nonuniform motion, J. Geophys. Res., 74, 3609-3627.

51. MIHALOV, J.D., COLBURN, D.S. and SONETT, C.P., 1970. Observations of the magnetopause geometry and waves at the lunar distance, Planet. Space Sci., 18, 239-258.

52. BEHANNON, K.W., 1968. Mapping of the Earth's bow shock and magnetic tail by Explorer 33, J. Geophys. Res., 73, 907-930.

53. SONNERUP, B.U.Ö. and CAHILL, L.J., Jr., 1967. Magnetopause structure and attitude from Explorer 12 observations, J. Geophys. Res., 72, 171-183.

54. SONNERUP, B.U.Ö. and CAHILL, L.J., Jr., 1968. Explorer 12 observations of the magnetopause current layer, J. Geophys. Res., 73, 1757-1770.

55. BURTON, R.K., McPHERRON, R.L. and RUSSEL, C.T., 1973. An empirical relationship between Dst and the solar wind electric field and dynamic pressure, Proc. Chapman Mem. Symp. Magnetospheric Motions, 139, Boulder, Colorado, June.

56. RUSSELL, C.T., 1975. The response of the magnetosphere to the solar wind, in "The Magnetospheres of Earth and Jupiter", 39-53, ed. Formisano,V., D. Reidel, Dordrecht, Netherlands.

57. RUSSELL, C.T. and McPHERRON, R.L., 1973. Semiannual Variation of Geomagnetic Activity, J. Geophys. Res., 78, 92-108.

58. RUSSELL, C.T., McPHERRON, R.L. and BURTON, R.K., 1974. On the cause of geomagnetic storms, J. Geophys. Res., 79, 1105-1109.

59. CHAPMAN, S. and BARTELS, J., 1940. Geomagnetism, chap. 11, Oxford University Press, New York.

60. MAYAUD, P.N., 1974. Comment on "Semiannual Variation of Geomagnetic Activity" by C.T. Russell and R.L. McPherron, J. Geophys. Res., 79, 1131.

61. RUSSELL, C.T. and McPHERRON, R.L., 1974. Reply, J. Geophys. Res., 79, 1132-1133.

62. VERCHEVAL, J., 1975. Un effet géomagnétique dans la thermosphère moyenne, Ann. Geophys., 31, 261-270.

63. McINTOSH, D.H., 1959. On the annual variation of magnetic disturbance, Phil. Trans. Roy. Soc. London, 251A, 525-552.

64. RUSSELL, C.T., 1971. Geophysical coordinate transformations, Cosmic Electrodynamics, 2, 184-196.

Figure 1 : Willis : The Micro-structure of the Magnetopause, Geophys. J.R. Astr. Soc. 41, 355-389, 1975, Fig. 1. p.356.

Figure 2 : Willis : idem, Fig. 3. p.359.

Figure 3 : Beard and Choe : The magnetospheric boundary, in "Correlated interplanetary and Magnetosph. Observations", Ed. D.E. Page, 1974, Fig. 3. p.101.

Figure 4 : Willis : idem, Fig. 4. p.363

Figure 5 : Willis : Structure of the Magnetopause, Rev. of Geophys. and Sp. Physics, 9(4), 953-985, 1971, Fig. 5. p.965.

Figure 6 : Roederer : Science, volume 183, Number 4120, 11 January 1974, 37-46, Fig. 2. p.39.

Figure 7 : Dessler : Solar wind interactions and the Magnetosphere, in "Physics of the Magnetosphere", Ed. R.L. Carovillano, J.F. McClay, H.R. Radoski, 65-105, 1968, Fig. 16. p.84.

Figure 8 : Cole : Outline of a theory of solar wind interaction with the magnetosphere. Planet. Space Sci., 22, 1075-1088, 1974, Fig. 1.p.1076.

Figure 9 : Willis : Structure of the Magnetopause, Rev. of Geophys. and Sp. Physics, 9(4), 953-985, 1971, Fig. 2. p.956.

Figure 10: Russell : The solar wind and Magnetospheric dynamics, in "Correlated interplanetary and Magnetospheric Observations", Ed. D.E. Page, 1974, Fig. 23. p.41.

Figure 11: Russell : idem, Fig. 22. p.39.

Figure 12: Russell : idem, Fig. 21. p.35.

Figure 13: Russell and McPherron, Semiannual variation of Geomagnetic Activity, J.G.R., 78(1), 92-108, 1973, Fig. 4. p.96.

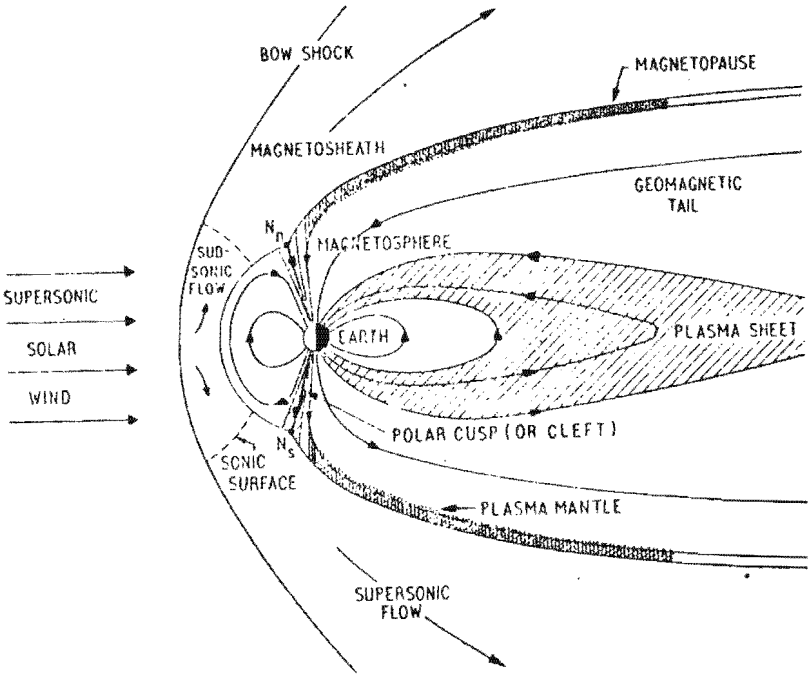

FIG. 1. A schematic illustration of the confined geomagnetic field and the detached bow shock wave in the noon-midnight magnetic meridian plane. This figure also delineates various regions of the Earth's plasma environment.

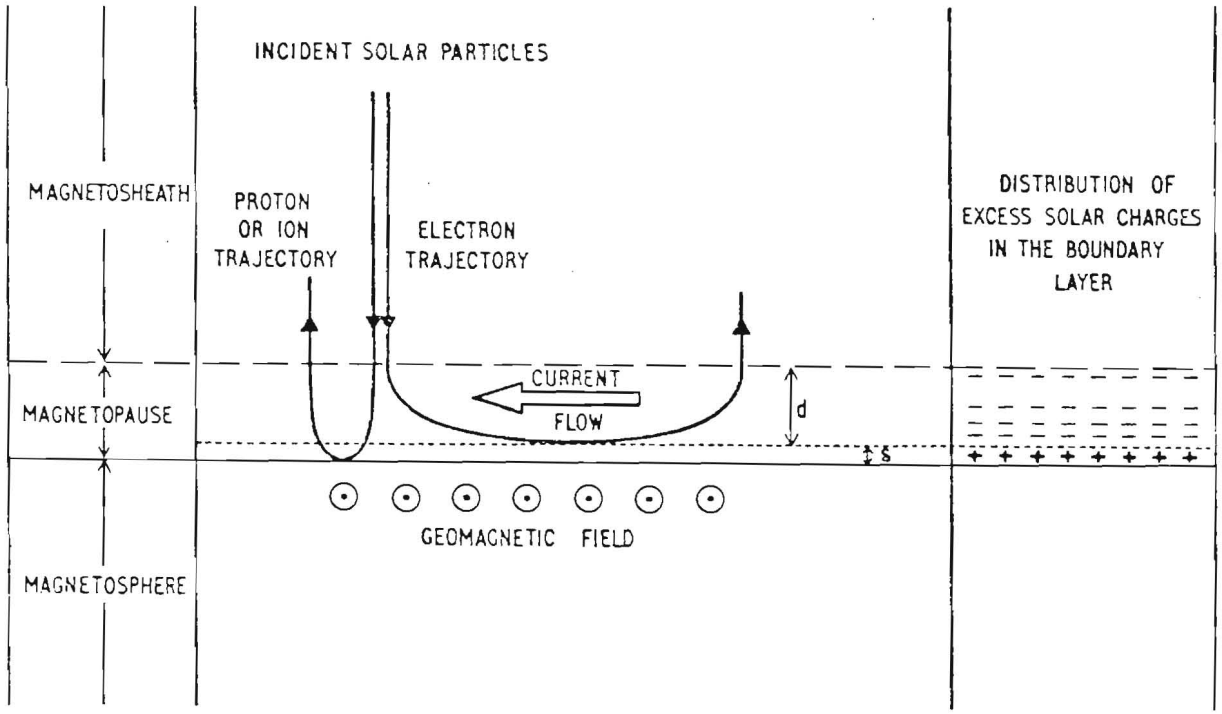

FIG. 2. A schematic illustration of the trajectories of magnetosheath ions and electrons incident normally on a plane boundary layer when the polarization electric field due to charge separation is present; $d \sim 1$ km, $\delta \sim 1$ m.

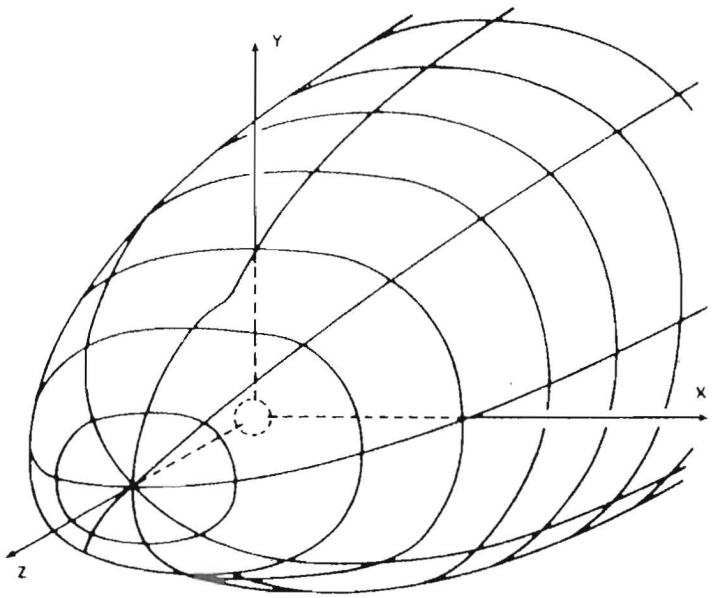

Fig. 3. Pictorial view of the magnetospheric boundary as computed by Midgeley and Davis.

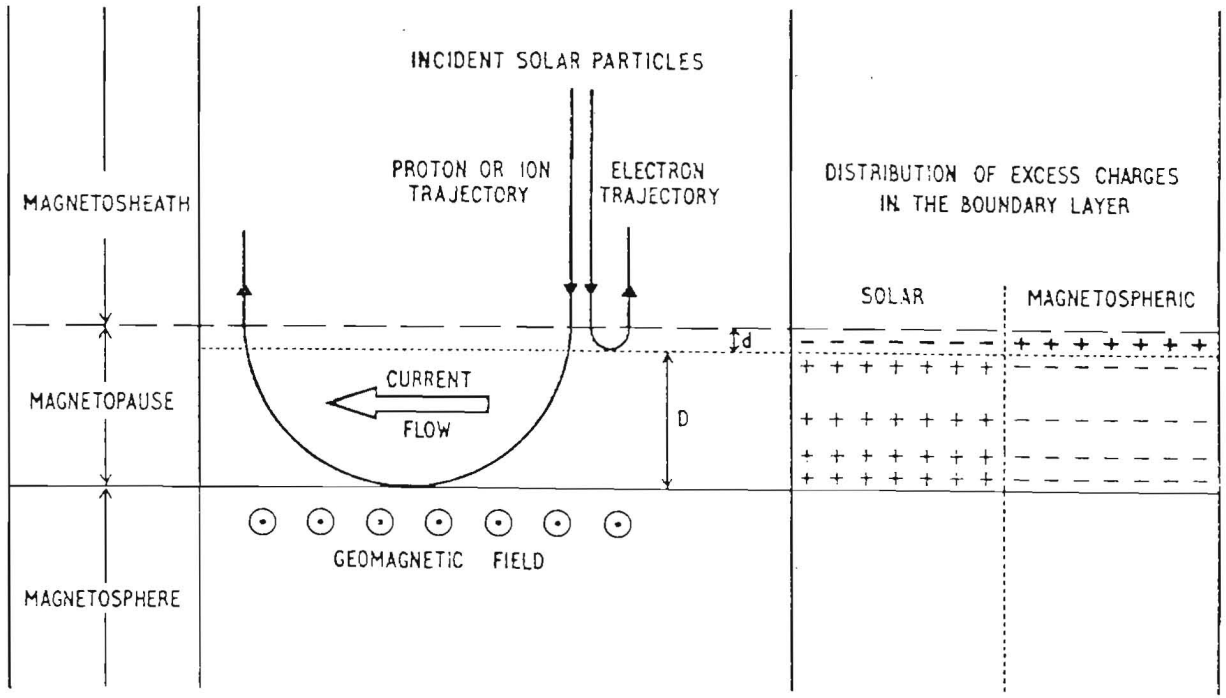

FIG. 4. A schematic illustration of the trajectories of magnetosheath ions and electrons incident normally on a plane boundary layer when the polarization electric field is completely neutralized by ambient magnetospheric charged particles; $D \sim 100$ km, $d \sim 1$ km.

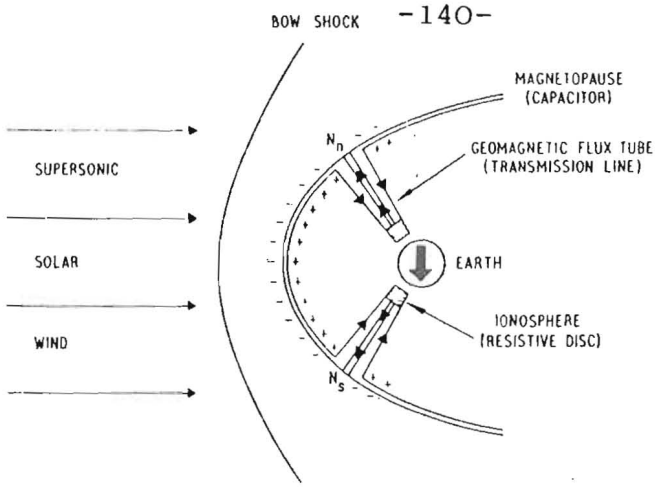

Fig. 5. A schematic illustration of the magnetosphere-ionosphere circuit. Also shown are the polarization charges at the magnetopause and the neutralizing currents that flow in the ambient plasma.

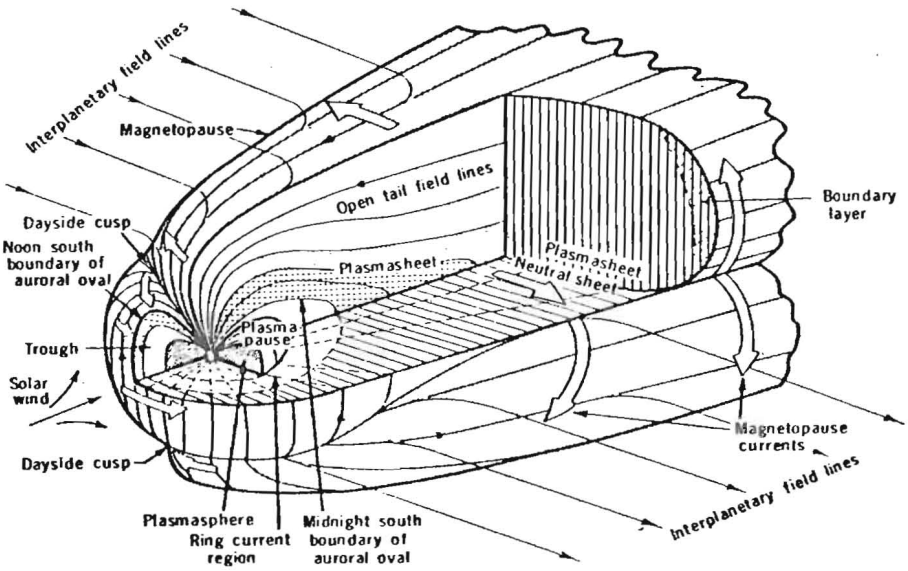

Fig. 6 Artist's conception of the magnetosphere, its plasma populations, and associated boundaries and currents (6).

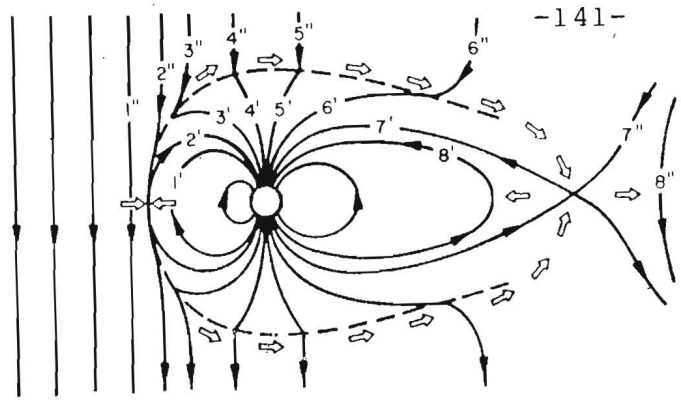

Fig. 7 Dungey's reconnection model of the magnetosphere.

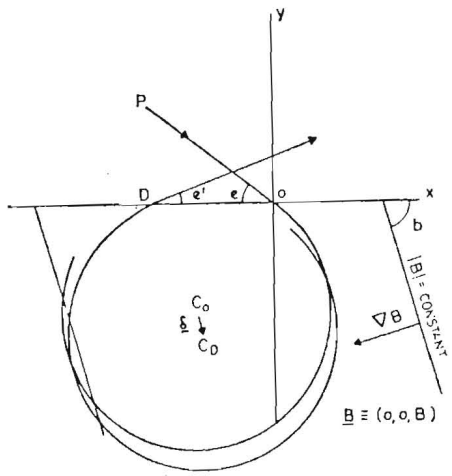

FIG 8 PROTON ENTERS MAGNETOSPHERE AT O WITH GUIDING CENTRE C_0 AND EXITS MAGNETOSPHERE AT D WITH GUIDING CENTRE AT C_D. NOTE THAT EXCEPT AT NOSE OF MAGNETOSPHERE ∇B IS NOT PERPENDICULAR TO THE MAGNETOPAUSE.

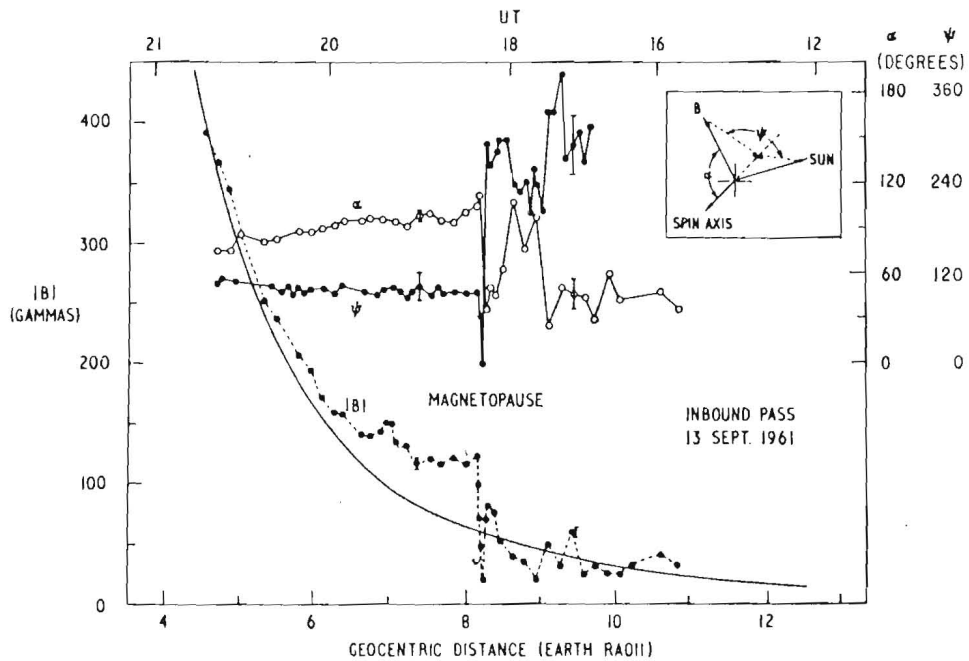

Fig. 9 A magnetometer record of the geomagnetic field obtained near the noon meridian during an inbound pass of Explorer 12 on September 13, 1961. The magnitude of the total magnetic intensity $|B|$ and the angles α and ψ, defined in the inset figure, are plotted against geocentric distance from the earth (1 gamma $= 10^{-5}$ gauss $= 10^{-9}$ Wb/m^2). The smooth curve shows the variation of $|B|$ with distance for the *Finch and Leaton* [1957] geomagnetic reference field. (After *Cahill and Amazeen* [1963].)

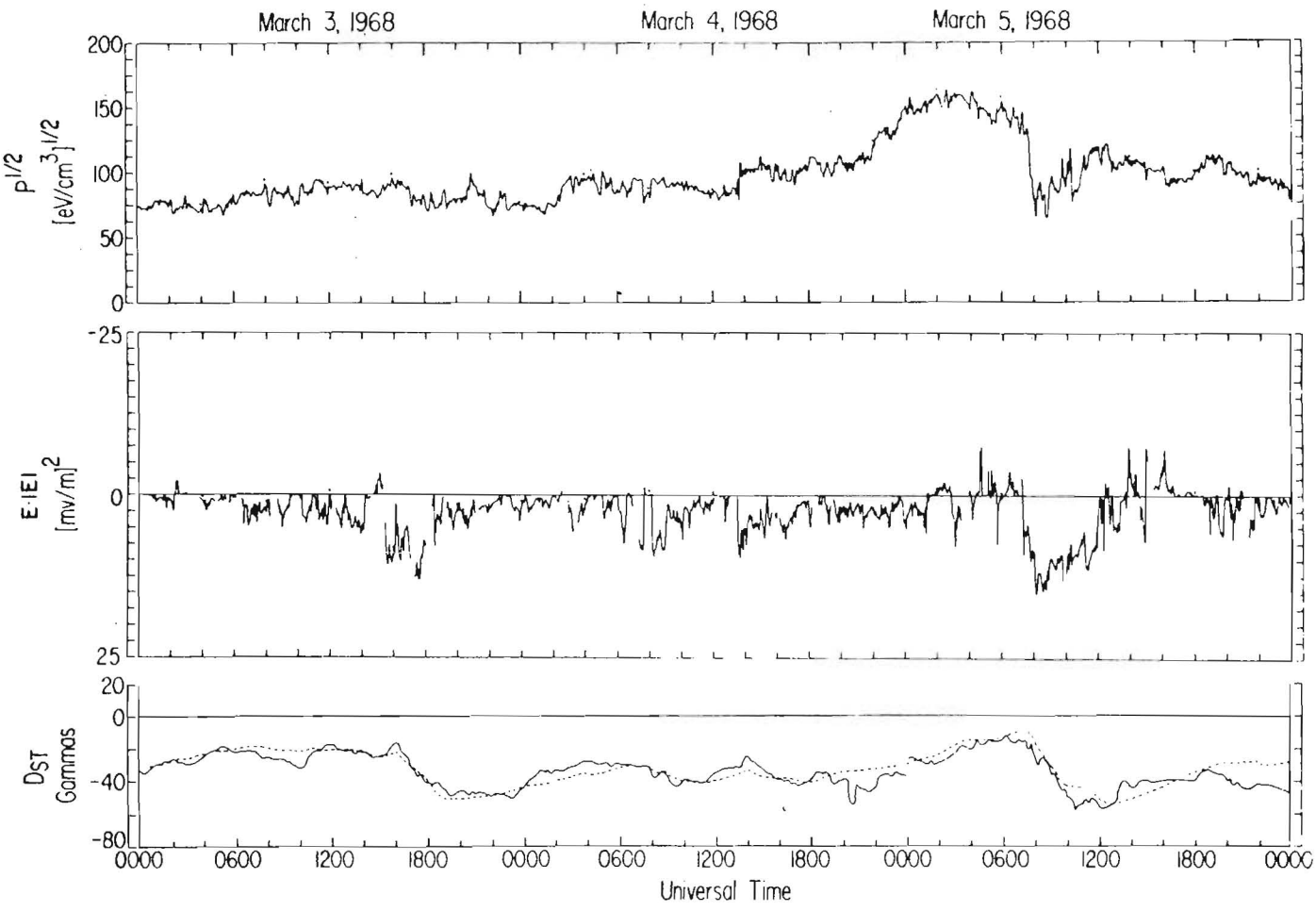

Fig 10 Prediction of Dst using solar wind dynamic pressure and interplanetary electric field. Top panel: square root of the dynamic pressure. Middle panel square of the westward solar magnetospheric component of the interplanetary electric field times its sign. Bottom panel: actual (solid line) and predicted (dashed line) Dst (Burton *et al.*, 1973).

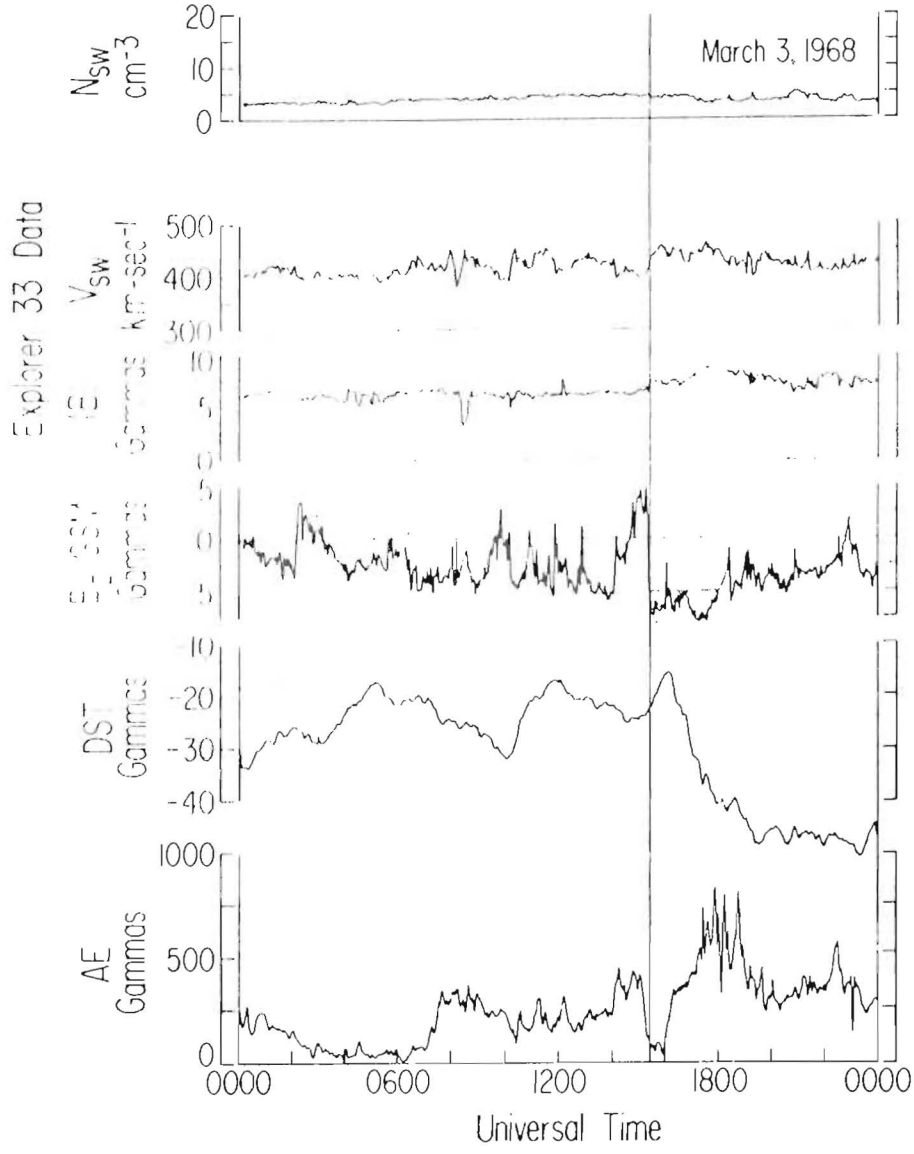

Fig **11** Solar wind and geomagnetic activity data for March 3, 1968. From top to bottom: the solar wind number density, N_{SW}, and the solar wind velocity, V_{SW}, measured by the MIT plasma probe on Explorer 33; the interplanetary field strength, $|B|$, and its solar magnetospheric Z-component, B_Z, as measured by the Ames Research Center fluxgate magnetometer on Explorer 33; 2.5 min evaluations of the Dst and AE indices (Russell *et al.*, 1973a).

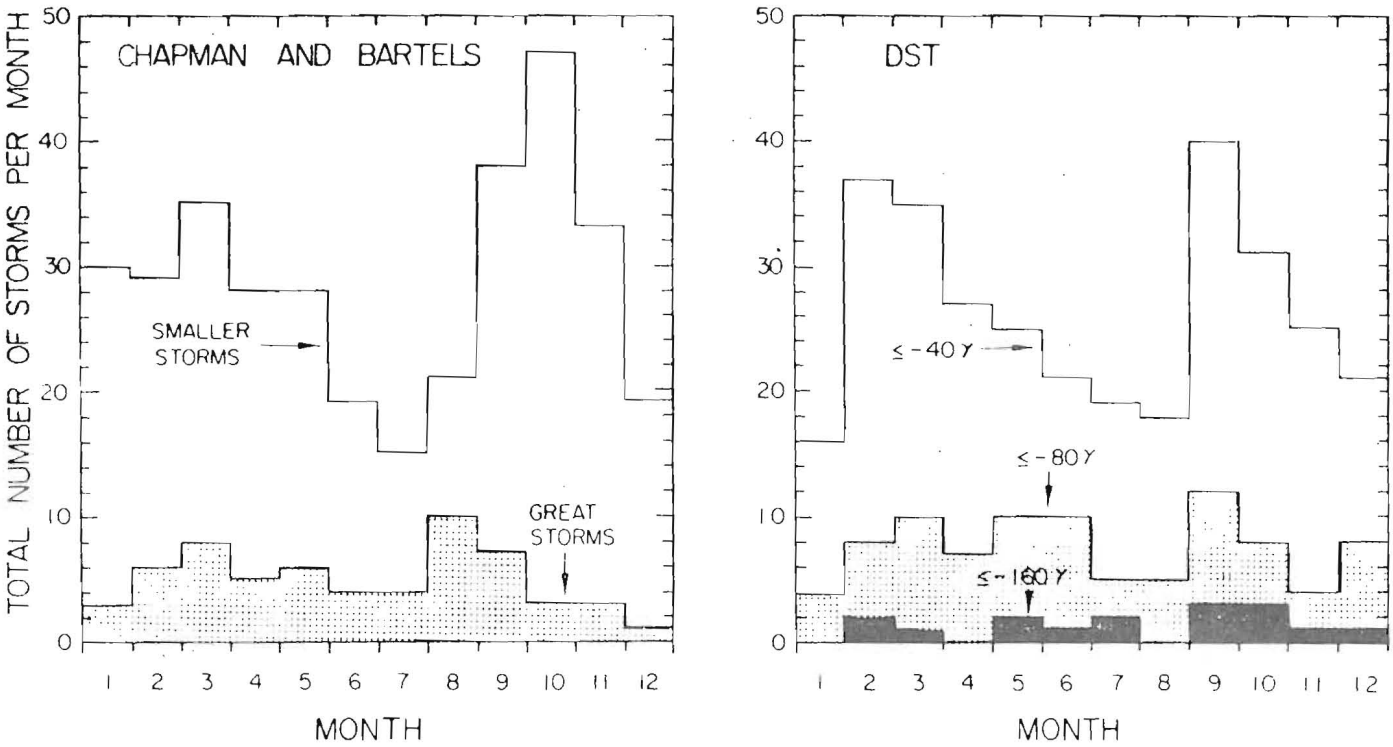

Fig. 12 The semiannual variation of the occurrence of geomagnetic storms. Left: occurrence of great storms and smaller storms from 1875 to 1927 given by Chapman and Bartels (1940). Right: occurrence of storms with Dst minimums less than −40, −80, and −160 γ during the years 1958 and 1961 through 1969 (Russell and McPherron, 1973b).

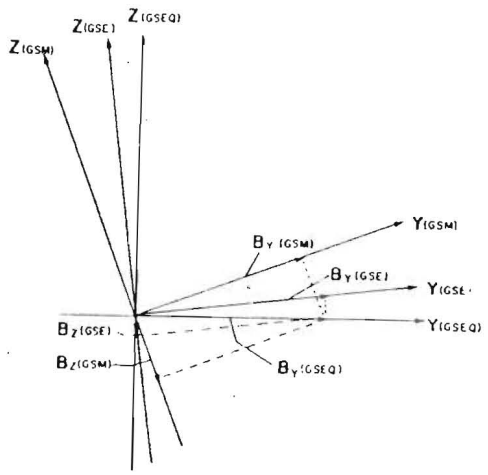

Fig. 13 One of the possible orientations of the Y-Z planes of the solar equatorial (GSEQ), solar ecliptic (GSE), and solar magnetospheric (GSM) coordinates, showing how a vector in the solar equatorial plane can have a southward (along the $-Z$ axis) GSE and GSM component.